Science of the Total Environment 795 (2021) 148872

Contents lists available at ScienceDirect

Science of the Total Environment

journal homepage: www.elsevier.com/locate/scitotenv

Predicting wildfire particulate matter and hypothetical re-emission of radiological Cs-137 contamination incidents

Kirk R. Baker [a,*], Sang Don Lee [a], Paul Lemieux [a], Scott Hudson [b], Benjamin N. Murphy [a], Jesse O. Bash [a], Shannon N. Koplitz [a], Thien Khoi V. Nguyen [c], Wei Min Hao [d], Stephen Baker [d], Emily Lincoln [d]

[a] U.S. Environmental Protection Agency, Research Triangle Park, NC, USA
[b] U.S. Environmental Protection Agency, Cincinnati, OH, USA
[c] U.S. Environmental Protection Agency, San Francisco, CA, USA
[d] Missoula Fire Sciences Laboratory, Rocky Mountain Research Station, US Forest Service, Missoula, MT, USA

HIGHLIGHTS

- This modeling system captures local to regional scale transport and levels of PM2.5 from wildfire.
- The model reasonably captured the extent of the surface mixing layer compared to measurements.
- Multiple hypothetical wildfire scenarios modeled with post-incident ^{137}Cs emissions.
- Modeled post-incident ambient levels ^{137}Cs would not require population evacuation or shelter-in-place.

GRAPHICAL ABSTRACT

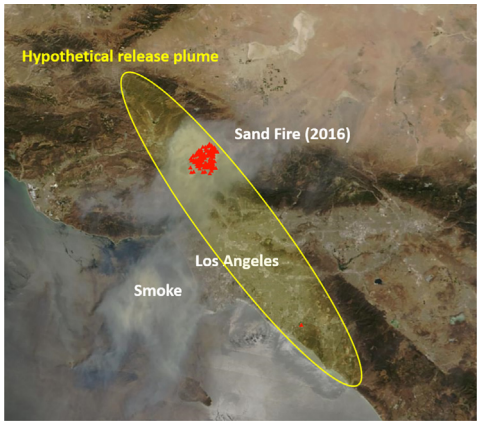

ARTICLE INFO

Article history:
Received 10 April 2021
Received in revised form 1 July 2021
Accepted 2 July 2021
Available online 5 July 2021

Editor: Elena Paoletti

Keywords:
Wildfire
Cesium
CMAQ
PM2.5

ABSTRACT

Radiological release incidents can potentially contaminate widespread areas with radioactive materials and decontamination efforts are typically focused on populated areas, which means radionuclides may be left in forested areas for long periods of time. Large wildfires in contaminated forested areas have the potential to reintroduce these radionuclides into the atmosphere and cause exposure to first responders and downwind communities. One important radionuclide contaminant released from radiological incidents is radiocesium (^{137}Cs) due to high yields and its long half-life of 30.2 years. An Eulerian 3D photochemical transport model was used to estimate potential ambient impacts of ^{137}Cs re-emission due to wildfire following hypothetical radiological release scenarios. The Community Multiscale Air Quality (CMAQ) model did well at predicting levels and periods of increased PM2.5 carbon due to wildfire smoke at routine surface monitors in California during the summer of 2016. The model also did well at capturing the extent of the surface mixing layer compared to aerosol lidar measurements. Emissions from a large hypothetical wildfire were introduced into the wildland-urban interface (WUI) impacted by a hypothetical radiological release event. While ambient concentrations tended to be highest near the fire, the highest population committed effective dose equivalent by inhalation to an adult from ^{137}Cs over an hour was downwind where wind flows moved smoke to high population areas. Seasonal variations in meteorology (wind flows) can result in differential population impacts even in the same metropolitan area. Modeled post-incident ambient levels of ^{137}Cs both near these wildfires and further downwind in nearby urban areas were well below levels that would necessitate population evacuation or warrant other protective

* Corresponding author.
E-mail address: baker.kirk@epa.gov (K.R. Baker).

https://doi.org/10.1016/j.scitotenv.2021.148872
0048-9697/Published by Elsevier B.V.

action recommendations such as shelter-in-place. These results suggest that 1) the modeling system captures local to regional scale transport and levels of PM2.5 from wildfire and 2) first responders and downwind population would not be expected to be at elevated risk from the initial inhalathion exposure of ^{137}Cs re-emission.
Published by Elsevier B.V.

1. Introduction

Wildland (wild and prescribed) fires have primary emissions of fine ($PM_{2.5}$) and coarse ("coarse PM") fraction particulate matter (Baker et al., 2016; Baker et al., 2018), both of which are known to negatively affect human health (Reid et al., 2016). Exposure to wildfire smoke is expected to increase in the future based on increased fuel availability and conducive meteorology (Abatzoglou and Williams, 2016; Schoennagel et al., 2017). Particulate matter emissions from wildland fires can include legacy pollutants that also have negative human health effects such as mercury (Wiedinmyer and Friedli, 2007), lead (Kristensen et al., 2014), and asbestos (Harper et al., 2015) in areas where these pollutants deposited in the past. Additionally, elevated levels of radiocesium (^{137}Cs) have been measured in biomass in areas impacted by radiological incidents (Takada et al., 2016; Yoschenko et al., 2006), and wildfire has been identified as a mechanism for environmental redistribution (Bourcier et al., 2010; Commodore et al., 2012; Paatero et al., 2009; Strode et al., 2012; Wotawa et al., 2006; Yoschenko et al., 2006).

Studies have shown ambient radionuclide concentration increased by multiple orders of magnitude compared to background levels during biomass burning in the area contaminated with ^{137}Cs from the Chernobyl power plant accident (Kashparov et al., 2000; Yoschenko et al., 2006). However, the levels observed and modeled were not considered significant in terms of inhalation exposure or a notable mechanism of terrestrial redistribution of radionuclides (Kashparov et al., 2000; Yoschenko et al., 2006). More recently, ^{137}Cs has been measured in biomass in areas impacted by the 2011 Fukushima Daiichi power plant accident (Hashimoto et al., 2012; Imamura et al., 2017). The amount of accumulated ^{137}Cs varies by biomass type and biomass form (leaves, litter, soil) (Hashimoto et al., 2012; Imamura et al., 2017; Tikhomirov and Shcheglov, 1994). Levels also vary by time elapsed since the accident and vary spatially due to proximity from the facility (Takada et al., 2016).

Nuclear power plant accidents, improvised nuclear device detonations, and radiological dispersal devices can introduce radionuclides into the environment, potentially contaminating large areas. ^{137}Cs is water soluble, has a long half-life (30.17 years), and can easily be taken up by plants (Zhu and Smolders, 2000). These properties mean a long residence time in soil and biomass contaminated by radiological incidents and thus increased re-emission potential during wildland fire activity (Garten Jr et al., 2000; Saffarzadeh et al., 2014). It is important to understand the potential post-incident impacts of ^{137}Cs from a typical wildfire to characterize exposure to support prioritization of post-incident remediation efforts (e.g., focus efforts on impacted urban, suburban, rural, or forested areas). Decontamination of forests is expensive and has negative ecosystem impacts through loss of habitat, soil erosion, and nutrient loss (Jouve et al., 1993; Linkov et al., 1997). Understanding potential exposure related to re-emission of ^{137}Cs during a wildfire could help determine whether potential negative human health impacts would necessitate remediation despite known negative ecosystem impacts related to forest decontamination.

Large wildfires in areas contaminated due to a radiological incident could result in significant exposure to first responders and downwind population areas depending on the amounts of radionuclides in consumed biomass, plume buoyancy, and meteorology (Goldammer et al., 2008; Hohl et al., 2012; Viner et al., 2015). Photochemical grid models have been shown to capture local (Zhou et al., 2018) to regional scale (Baker et al., 2018) wildfire plume transport (e.g., plume buoyancy and meteorologically driven transport) and skill in estimating surface level components of particulate matter for large wildfires (Baker et al., 2016; Baker et al., 2018). Here, a photochemical grid model was applied to estimate 1) actual downwind $PM_{2.5}$ and coarse PM wildfire impacts in California during the summer of 2016 which had notable wildfire activity and 2) use that platform to test hypothetical scenarios where wildfires caused re-emission of legacy ^{137}Cs. The hypothetical scenarios involve modeling downwind ^{137}Cs concentrations and exposure to nearby populated areas from large (but not extreme) wildfires emitting ^{137}Cs from hypothetical past radiological incidents in Los Angeles and Denver developed for multi-agency emergency response planning. Wildfire emissions of ^{137}Cs were based on laboratory testing and modulated to reflect anticipated post-incident levels of ^{137}Cs in biomass. The inhalation exposure pathway was estimated for each of these hypothetical scenarios using conservative assumptions to determine whether ^{137}Cs re-emission during a wildfire would necessitate people exposed downwind to wear personal protection equipment or shelter in place.

This study intends to show that a regional scale application of a photochemical grid model provides a reasonable representation of the timing and level of PM2.5 impacts of smoke from wildfire in the western U.S. Model performance will be based on model predictions of surface level PM2.5 compared to routine surface level measurements of speciated PM2.5 during a period of wildfire activity in California during 2016. Second, the modeling system will have a wildfire augmented with hypothetical ^{137}Cs emissions to estimate downwind ambient ^{137}Cs and committed effective dose equivalent. The objective is to understand whether levels are high enough to warrant shelter-in-place warnings for people exposed to wildfire smoke in situations where a past radiological event had contaminated the fuel.

2. Methods

2.1. Modeling system description and application

The Community Multiscale Air Quality (CMAQ) modeling system version 5.3.2 (doi: https://doi.org/10.5281/zenodo.4081737) was used to model wildfire ^{137}Cs impacts and has been applied extensively to estimate local to regional scale coarse (Li et al., 2013; Nolte et al., 2015) and fine fraction PM (Appel et al., 2013; Nolte et al., 2015). CMAQ was applied using 4 km sized grid cells for domains covering California and Colorado (Fig. S1). A total of 35 layers were used to resolve the vertical atmosphere from the surface to 50 mb with more layers near the surface to best resolve diurnal variation in the surface mixing layer. Meteorological inputs to CMAQ were generated using version 3.7 of the Weather Research and Forecasting (WRF) model (Skamarock et al., 2005). WRF and CMAQ were applied with the same Lambert conic conformal grid projection. CMAQ was also applied using 1 km sized grid cells for a smaller area around each of the hypothetical fires. Meteorological inputs for the 1 km simulations were interpolated from the coarser 4 km meteorology.

Anthropogenic emissions were based on the 2014 National Emission Inventory (U.S. Environmental Protection Agency, 2018) and processed for input to CMAQ using the Sparse Matrix Operator Kernel Emissions (SMOKE) model (DOI: https://doi.org/10.5281/zenodo.1321280). Biogenic emissions were estimated with the Biogenic Emission Inventory System (BEIS) version 3.6.1 using temperature and solar radiation estimated by the WRF model (Bash et al., 2016). Previous work has shown that anthropogenic (Baker et al., 2015) and biogenic (Bash et al., 2016) emissions are generally well characterized in southern California and Denver region (Kelly et al., 2016). Spatial and time variant

chemical species inflow were based on an annual CMAQ simulation covering the contiguous United States. Wildland fire emissions were day specific and based on incident information and satellite fire detections for actual fire location and size (Baker et al., 2016; Larkin et al., 2020).

Model predictions of $PM_{2.5}$ organic carbon and coarse PM (unspeciated) were paired with measurements at rural monitors in California in 2016 when wildfire activity was present in the area to demonstrate model skill in capturing fire-receptor relationships. Hourly model predictions were converted to local time and aggregated to daily average and matched with daily average measurements taken every 3 days. $PM_{2.5}$ organic carbon is used as an indicator for wildfire smoke because it is the largest chemical component, and rural non-coastal monitors are used to minimize the influence of model performance related to anthropogenic or other geogenic (e.g., sea salt) emissions sources. Coarse PM mass performance is included since the hypothetical scenarios include coarse PM impacts.

Special instruments deployed as part of field study efforts in California in 2016 (Faloona et al., 2020) and in Denver in 2014 (Flocke et al., 2020) provide information about the height of the surface mixing layer and an indication about how well the model is representing this important parameter for surface level concentration estimates (Langford et al., 2019; Senff et al., 2020). The ceilometer deployed in Denver has a gradient-based algorithm that is part of Vaisala's ceilometer data logging software that calculates 3 mixed-layer heights and up to 3 cloud levels (Knepp et al., 2017). In addition to surface mixing layer height prediction, a visual examination of vertical gradients in aerosol measured by these instruments provides a strong indication about the height of the surface mixing layer. Model skill in representing smoke transport is based on a comparison of model predicted winds with those measured at routine National Weather Service surface monitors.

2.2. Incident scenarios

CMAQ was applied for the period of July 1 to 13, 2014 for the Denver scenario and May 15 to October 1, 2016 for the Los Angeles scenario. The 2014 period was selected for Denver to take advantage of a field campaign (Flocke et al., 2020) that provided unique measurements of surface layer mixing height useful for evaluating model vertical mixing of pollutants. The 2016 period was chosen for California because a field campaign provided information about the vertical structure of aerosol from smoke plumes using lidar technology (Langford et al., 2019; Senff et al., 2020) and because that summer featured large wildfires near Los Angeles that could serve as a basis of the hypothetical scenarios. A summer and fall episode were extracted from the California scenario to focus on different seasons with winds blowing toward the Los Angeles area.

Each hypothetical wildfire was modeled for each day of the simulation. Wildfire impacts were estimated as the difference between a baseline simulation with all sources and a second simulation with all sources with the hypothetical wildfire. The California hypothetical scenarios was based on the actual emissions and location of the Sand fire (located to the north of Los Angeles in 2016), with radionuclides artificially included in the emissions. The wildfire in the Denver scenario is based on the actual Sand fire (same as the California scenario) but the location is hypothetical (located just west of Denver).

The Denver scenario (Fig. S2) was based on a hypothetical truck-dirty-bomb incident developed for the 2012 Wide Area Recovery and Resiliency Program (WARRP). WARRP was an interagency initiative intended to reduce time and resources required to remediate urban areas following a catastrophic chemical, biological, or radiological incident (Connell, 2012). The original radiological incident plume impacts were based on southerly winds. The impact plume orientation was modified for this hypothetical scenario by assuming winds were out of the east during the hypothetical radiological incident so that the ^{137}Cs release impacted forested areas in the foothills west of Denver where wildfire has happened in the past and would be possible in the future (Dennison et al., 2014).

The Los Angeles scenario was based on a hypothetical nuclear power plant incident (Fig. S2). In this situation, winds blew a narrow plume from the facility location south of Los Angeles toward the northwest impacting Los Angeles and mountains north of the city. The downwind impacted area includes the location of the 2016 Sand fire (https://en.wikipedia.org/wiki/Sand_Fire_(2016)) and the amount deposited was assumed to be the same as the WARRP scenario since emissions and deposition information are not publicly available for this scenario.

2.3. Laboratory ^{133}Cs emissions

PM Cs emissions were based on a laboratory study that examined the partitioning of ^{133}Cs (a stable, non-radioactive isotope of Cs) between airborne particulate matter and residual non-entrained ash when pine needles and peat were doped with Cs (Hao et al., 2018). ^{133}Cs has identical chemical and physical properties as ^{137}Cs but does not have the same negative human health effects. Table 1 provides information used to generate PM ^{133}Cs emissions, which include laboratory experiments measuring fuel, ^{133}Cs content of the fuel, and ^{133}Cs measured in the air as a rate of mass per fuel burned (g ^{133}Cs/kg litter burned). Table 1 includes measurements reported in Hao et al., (2018) and additional measurements performed in 2018 at the same facility following methods described in Hao et al., (2018). The 2018 laboratory measurements were done with more intense fire to generate more smoke and higher pollutant levels to exceed the lower threshold for instrument detection capability. The highest emissions estimate for fine and coarse fraction PM was selected for the hypothetical wild fire to provide a conservative estimate of ^{137}Cs impacts (Hao et al., 2018). The highest measured emissions of $PM_{2.5}$ ^{133}Cs per fuel consumed was 0.006 g/kg and 0.008 g/kg for coarse PM mode (Table 1). Other experimental studies have shown ^{137}Cs in the fine fraction of PM when pine needles were burned and also in the coarse fraction (and larger) as a component of ash (Kashparov et al., 2000).

2.4. Modeled ^{137}Cs emissions

The fraction of Cs in the fuel was much higher for the laboratory testing compared to actual post-incident levels to ensure detectable levels using conventional measurement methods that are appropriate for non-radioactive metals (Hao et al., 2018). For modeling purposes, laboratory-based PM ^{133}Cs emission factors were adjusted downward based on a simple approximation of ^{137}Cs deposition from the Denver hypothetical WARRP radiological release scenario (Connell, 2012). This adjustment was checked for reasonableness with a comparison with multiple sources of post-incident ^{137}Cs litter fuel contamination levels measured near Fukushima and Chernobyl.

The WARRP radiation incident scenario had a total release amount of 8.5×10^7 MBq. Assuming uniform deposition across the impacted area would result in approximately 1,000,000 Bq/m^2 or 0.31 g ^{137}Cs/km^2 (Eq. S1) which is comparable to the largest measurement downwind of multiple nuclear facility incidents. Post-incident ^{137}Cs litter biomass contamination values measured near Fukushima and Chernobyl vary depending on the time elapsed since the incident and proximity to incident. Values ranged from 13,000 Bq/m^2 (Takada et al., 2016) to 880,000 Bq/m^2 (Kashparov et al., 2000). The highest value in this range was selected to be conservative in the estimation of exposure. The 880,000 Bq/m^2 was converted to 0.273 g of ^{137}Cs per km^2 for comparison to laboratory fuel measurements (Eq. (S1)).

Laboratory estimates of Cs in pine needle fuel (litter) were 1.4 to 2.3 g Cs/kg litter (Hao et al., 2018) with an average of 1.8 g/kg (Table 1). An estimate of 0.05 tons litter per km^2 for the areas of the hypothetical fires near Denver and Los Angeles was extracted from the U.S. Forest Service's Fuel Characteristics Classification System (FCCS) v2 module (U.S. Forest Service, 2019). A similar value of 0.04 tons litter/

Table 1
^{133}Cs emissions and fuel content for laboratory burns done in March 2016 (Hao et al., 2018) and February 2018.

Run	Fuel type	Fuel measurements				Ambient $PM_{2.5}$			Ambient Coarse PM		
		Fuel Weight (kg)	Fuel Burned (kg)	Cs Fuel Weight (g)	Cs per Fuel Weight (g/kg)	Total Cs in $PM_{2.5}$ (g)	Cs emitted of total fuel burned (g/kg)	% Cs emitted of Cs fuel	Total Cs in coarse PM (g)	Cs emitted of total fuel burned (g/kg)	% Cs emitted of Cs fuel
March 2016 run 6	Pine needle	5.55	5.2	9.6	1.7	0.03	0.006	0.004	0.00	0.000	0.00
March 2016 run 7	Pine needle	5.24	4.9	13.3	2.5	0.000	0.000	0.000	0.00	0.000	0.00
March 2016 run 8	Pine needle	5.16	4.8	10.8	2.1	0.000	0.000	0.000	0.00	0.000	0.00
Feb 2018 run 1 (blank)	Pine needle	6.65	6.35	0.04	0.0066	0.000	0.000	0.000	0.00	0.000	0.00
Feb 2018 run 2 (blank)	Sage	5.82	5.60	0.05	0.0085	0.000	0.000	0.000	0.00	0.000	0.00
Feb 2018 run 3	Pine needle	6.29	5.84	8.81	1.4	0.000	0.000	0.000	0.00	0.000	0.00
Feb 2018 run 4	Pine needle	6.29	5.79	8.81	1.4	0.000	0.000	0.000	0.00	0.000	0.00
Feb 2018 run 5	Pine needle	6.32	5.85	8.84	1.4	0.000	0.000	0.000	0.05	0.008	0.52
Feb 2018 run 6	Sage	6.15	5.91	9.84	1.6	0.000	0.000	0.000	0.00	0.000	0.00
Feb 2018 run 7	Sage	6.20	5.94	14.26	2.3	0.000	0.000	0.000	0.00	0.000	0.00
Feb 2018 run 8	Sage	5.80	5.51	9.87	1.7	0.000	0.000	0.000	0.04	0.008	0.46

km^2 was measured for forests near Chernobyl (Yoschenko et al., 2006). Multiplying 1.8 g/kg by 0.05 tons litter per km^2 results in 5,224,320 g ^{137}Cs/km^2 (Eq. (S2)), which is a factor of approximately 2×10^7 higher than the Denver WARRP scenario and post-incident measurements. This factor is also similar to the ratio of ^{137}Cs measured in litter downwind of Chernobyl compared to laboratory fuel levels (Kashparov et al., 2000).

Above-ground biomass and soil have also been shown to be long-term reservoirs of ^{137}Cs after a radiological contamination event (Hashimoto et al., 2012; Tikhomirov and Shcheglov, 1994). Measurements of ^{137}Cs in above-ground biomass, litter, and soil at nine locations impacted by the Fukushima incident over 5 years (Imamura et al., 2017) show litter contains on average 20 to 47% of total contamination of the 3 reservoirs of ^{137}Cs and tends to decrease over time (Table S1).

Modeled emissions of ^{137}Cs were reduced by a factor of 2×10^7 to minimize the influence of laboratory fuel doping and be comparable to post-incident levels in litter. Emissions from above-ground biomass and soil were considered the same as litter for the purposes of this study since laboratory measurements of ^{137}Cs in PM were only available for litter and multiple studies indicate ^{137}Cs would be present in other biomass components (Imamura et al., 2017; Kashparov et al., 2000). This assumption is conservative for these hypothetical scenarios since the amount of ^{137}Cs in fuel will decrease over time. The Sand wildfire near Los Angeles burned ~45 km^2 per day with a daily total of 767 μg $PM_{2.5}$ ^{137}Cs and 1023 μg of coarse PM ^{137}Cs emissions artificially added to the fire emissions profile to reflect re-emission of hypothetical legacy incidents.

2.5. Exposure pathways

The exposure pathway considered in this assessment is inhalation using conservative assumptions that would be considered protective of the broader population. For instance, the ventilation rate of a healthy working male is used because that rate is higher than other population groups and would result in a more conservative estimate of dose rate for comparison to levels that would require action to be taken to minimize exposure. The dermal exposure route is not considered here because that route results in little uptake into the human body (Eckerman et al., 1988). Ingestion of contaminated foodstuffs was not considered in this assessment. A reasonable assessment of the ingestion pathway would require understanding the spatial nature of agriculture in these areas and how that food is distributed locally and nationally along with information about food consumption. Long term exposure from deposited radiocesium is not estimated for this hypothetical exercise.

Modeled ambient concentrations were converted to an estimate of committed effective dose equivalent (CEDE) by inhalation to an adult from ^{137}Cs over an hour using Eq. (1). The CEDE is a function of the modeled ^{137}Cs concentration, specific activity factor, standard reference breathing rate for an adult, and dose per intake from inhalation factor. When interpreting these results, it is important to recognize physiological differences between workers and general public (e.g., sensitive subpopulations, children).

$$CEDE\left(\frac{Sv}{hr}\right) = Modeled\ 137Cs\ \frac{\mu g}{m^3}\left(\frac{g}{10^6\ \mu g}\right)\left(\frac{3.2 \times 10^{12} Bq}{g}\right) \times \left(\frac{0.96\ m^3}{hr}\right)\left(\frac{3.9 \times 10^{-8}\ Sv}{Bq}\right) \quad (1)$$

The number for "pure" ^{137}Cs specific activity is 3.2×10^6 MBq/g (Browne and Tuli, 2007). The standard reference breathing rate for an adult was 0.96 m^3/h and inhalation dose coefficient of 0.039 μSv/Bq for ^{137}Cs (IAEA, 2011). CEDE was estimated for each grid cell and hour of the simulation.

2.6. Deposition

CMAQ was applied with wet and dry deposition processes represented using hourly input meteorology (Appel et al., 2020). Modeled deposition estimates of ^{137}Cs were converted from kg/ha to Bq/m^2 for comparison with values provided in literature (Eq. (S3)).

3. Results & discussion

Downwind impacts follow the wind patterns in each region. Since these scenarios are hypothetical, ambient measurements are not available to evaluate how well the modeling system predicts ^{137}Cs. The modeling system is being used to provide a conservative estimate of ^{137}Cs inhalation exposure from hypothetical scenarios where deposition from past incidents is released into the atmosphere by wildfire. First, the modeling system skill in predicting wildfire smoke and surface level concentration was assessed. This includes evaluation of horizontal and vertical transport using routine surface measurements of $PM_{2.5}$ carbon, winds (speed and direction), and special field study measurements of boundary layer mixing height. Second, the modeling system was applied to predict impacts of hypothetical legacy ^{137}Cs from wildfire activity. Ambient concentrations and deposition predicted by the modeling system is shown along with an estimate of CEDE through the inhalation pathway.

3.1. Modeling system skill in wildfire smoke prediction

Daily average model predicted $PM_{2.5}$ organic carbon is paired with surface level ambient measurements made at monitors likely impacted

by wildfire smoke in California during 2016 (Fig. 1). These plots show that the model does well at capturing the periods of wildfire impacts at these monitors. The model both over and underpredicts $PM_{2.5}$ organic carbon during these periods and does not have an obvious systematic bias. Coarse mass predictions do not match well with ambient data at these same locations (Fig. S3). The ambient measurements of coarse mass do not appear to follow the same temporal (day to day) pattern as $PM_{2.5}$ organic carbon which suggests these sites may not be close enough to wildfire activity to have elevated coarse mass. Based on the differences in concentration and temporal patterns of ambient measurements of coarse mass at these sites it appears these areas are dominated by emissions sources, some of which not well characterized by the modeling system, other than wildfire during this time period. The difference in performance for PM2.5 and coarse mass is most likely due to the routine surface monitors used for model performance may not be close enough to a large wildfire to have an impact above typical conditions while PM2.5 can impact monitors much further downwind due to the longer atmospheric residence time.

Winds (speed and direction) were well characterized based on surface measurements during these periods (Figs. S4 and S5). The good agreement between model and observed winds is also evident in the modeling system typically capturing periods of elevated $PM_{2.5}$ carbon at monitors when wildfire impacts were likely at these locations (Fig. 1). The height of the surface mixing layer is also important for predicting surface level concentrations. The meteorological model used for this analysis has been shown to compare well with surface mixing layer height measurements made as part of a special field campaign in the Los Angeles area (Baker et al., 2013). The model compares well with observed daytime surface mixing layer heights and tends to underestimate the extent of vertical mixing overnight in the Denver area during the 2014 modeling period (Fig. S6). Fig. 2 shows the vertical profile of aerosol backscatter measured in central California during 2016 compared with the vertical profile of model predicted $PM_{2.5}$ carbon. During this period where wildfire smoke passed over the lidar (Langford et al., 2019), the modeling system did well at predicting the boundary layer mixing height and to some extent the different stratified layers of smoke transported from wildfires to the north.

3.2. Hypothetical scenarios: ambient and deposition impacts

The episode maximum hourly $PM_{2.5}$ concentrations of ^{137}Cs for the Denver and Los Angeles hypothetical scenarios are shown in Fig. 3.

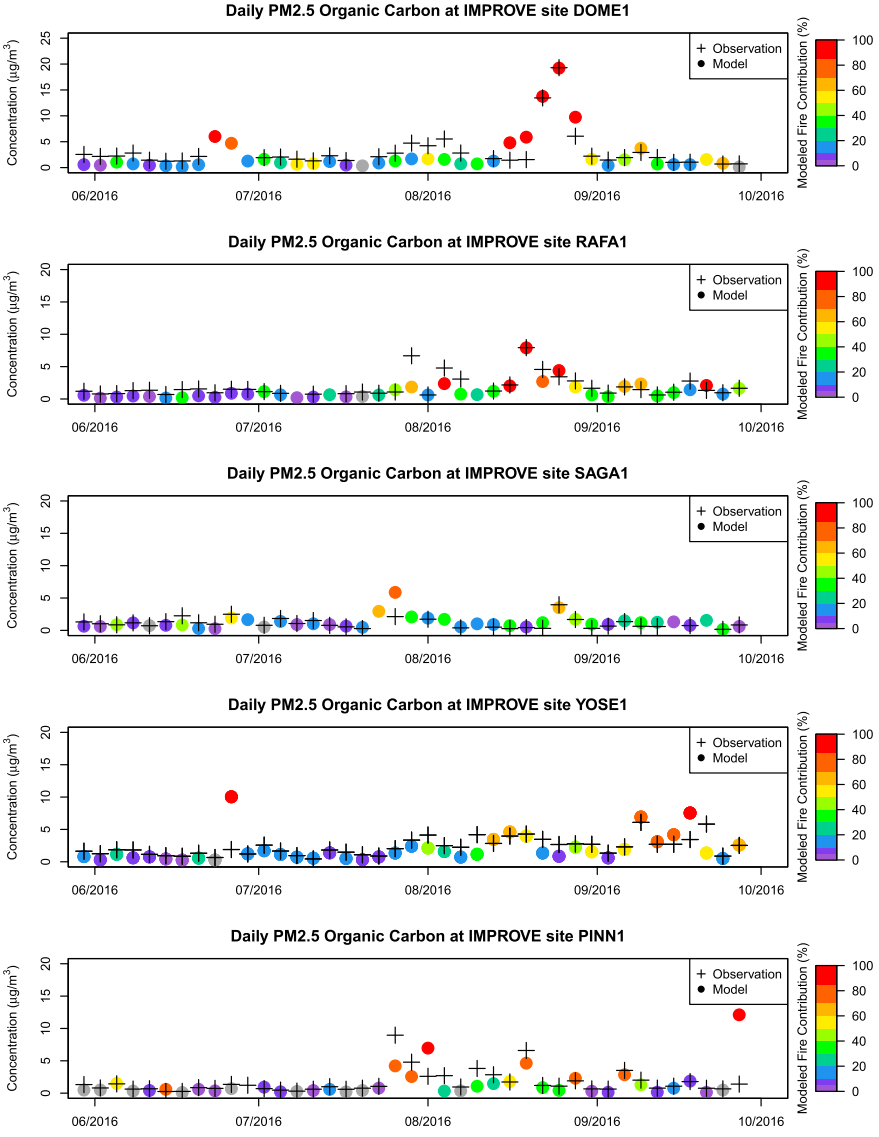

Fig. 1. $PM_{2.5}$ organic carbon measurements and model predictions shown at multiple rural monitor locations in California during 2016 that were impacted to some degree by wildfire smoke. Model predicted $PM_{2.5}$ organic carbon is shaded by the relative amount of total $PM_{2.5}$ organic carbon attributed to wildfire emissions. Fig. S-1 shows the location of these monitors.

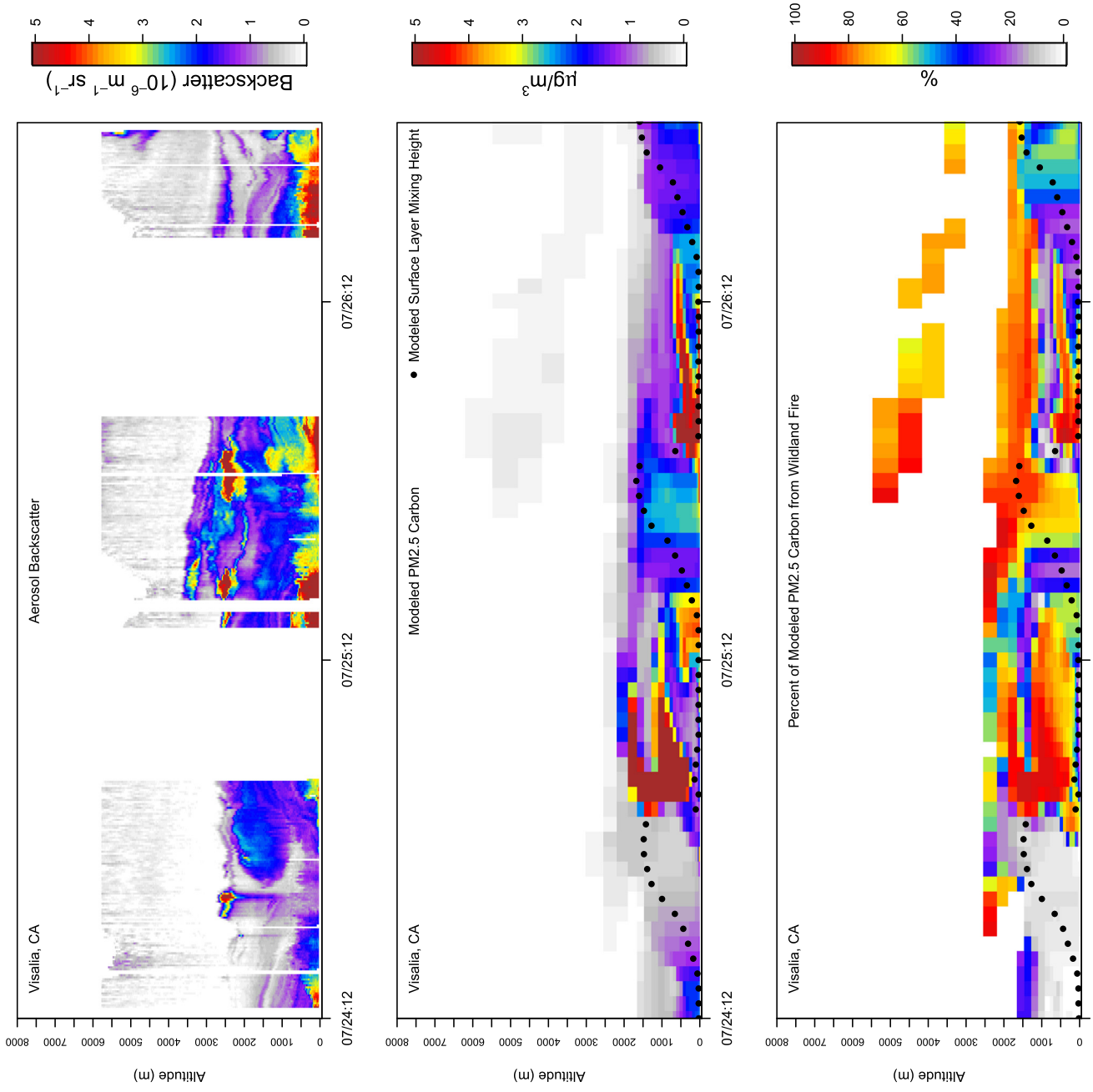

Fig. 2. Vertical profile of measured aerosol backscatter (top), modeled $PM_{2.5}$ carbon (middle), and percent of model predicted $PM_{2.5}$ carbon attributed to wildfire activity (bottom) at Visalia, CA between July 24 and 27, 2016.

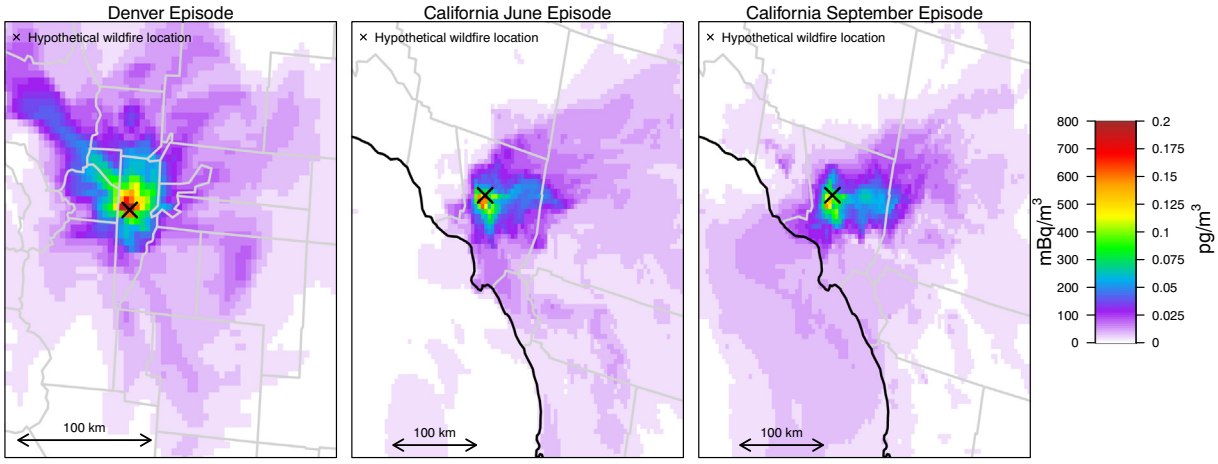

Fig. 3. Episode maximum modeled hourly ambient concentration for $PM_{2.5}$ cesium-137 for the Denver scenario and both Los Angeles scenarios.

The maximum hourly modeled ambient and deposition levels 50 km from the fire are shown in Table 2. The average of the maximum hourly modeled ambient and deposition levels within 50 km of these fires is also shown in Table 2. As expected, concentrations are highest near the fire and tend to decrease as distance from the fire increases (Fig. 4). Coarse mode ^{137}Cs concentrations (370 mBq/m^3 hourly maximum for Los Angeles scenario and 588 mBq/m^3 hourly maximum for Denver scenario) were slightly higher than fine mode concentrations (258 mBq/m^3 hourly maximum for Los Angeles scenario and 459 mBq/m^3 hourly maximum for Denver scenario) near the fire. Ambient concentrations of fine and coarse mode ^{137}Cs are similar in magnitude and pattern of downwind impact. The coarse PM levels then decrease more quickly as distance from the source increases compared to $PM_{2.5}$ due to the greater dry deposition velocity (Appel et al., 2020; Nolte et al., 2015). The larger near-fire contribution of coarse sized particles to ^{137}Cs is consistent with measurement studies done downwind of wildfire smoke contaminated with ^{137}Cs (Kashparov et al., 2000).

Since ^{137}Cs measurements are not available due to the hypothetical nature of this modeling assessment, published ambient concentration and deposition levels made as part of field measurements or model assessments of wild or prescribed fires contaminated with ^{137}Cs provide some context for model predictions from these scenarios. One modeling study presented near-fire measured ambient concentrations ranging between 0.1 and 1 Bq/m^3 from the fire location downwind to 350 m from a prescribed forest fire contaminated with ^{137}Cs from Chernobyl (Yoschenko et al., 2006). Another field study measured time integrated ambient ^{137}Cs at levels ranging from 10 to 100 mBq/m^3 with highest concentrations at the furthest measurement point (270 m) from the fire (Kashparov et al., 2000). A modeling study presented ^{137}Cs integrated concentrations estimated from contaminated prescribed fires at levels between 100 and 500 Bq s/m^3 at 4 to 8 km downwind of those fires, which represent a distance more comparable with the grid resolution used in this assessment (Kashparov et al., 2000). Another modeling study predicted concentrations up to 47 Bq/m^3 in wildfire smoke with highest levels nearest the fire (Hohl et al., 2012). The near-fire predictions of ambient ^{137}Cs for the scenarios modeled here were generally lower than other studies using models to estimate this contaminant in wildfire smoke. This could be related in part to different levels of ^{137}Cs in the fuel, different emission rates, coarser grid resolution used in this study, different approaches for aggregating plume concentrations over time and space, or some combination of these and other factors.

Model-predicted total deposition through the dry pathway is shown for each scenario in Fig. 5. The wet pathway is not shown since extensive rainfall would either extinguish the fire or result in significantly lower emissions in an actual scenario. Deposition of ^{137}Cs is highest near the fire and decreases as distance from the fire increases (Fig. S7). Most of the near-fire deposition is in the form of coarse fraction particulate since the deposition velocity for coarse particles is much larger than fine particles. Maximum predicted coarse model deposition was 1118 Bq/m^2 (mean = 52 Bq/m^2) for Los Angeles scenarios and 4475 Bq/m^2 (mean = 123 Bq/m^2) for the Denver scenario. Fine fraction deposition totals were much lower for each scenario (max = 82 Bq/m^2 for Los Angeles and max = 217 Bq/m^2 for Denver).

Other studies that have made near-fire field deposition measurements of ^{137}Cs deposition found ~10 Bq/m^2 at 50 to 500 m downwind of a prescribed fire contaminated by ^{137}Cs (Yoschenko et al., 2006). A model-based assessment of ^{137}Cs deposition from a contaminated wildfire near Chernobyl suggests a peak level of 110 Bq/m^2 at 1.5 to 2 km downwind (Kashparov et al., 2000). While not explicitly detailed in these references, the values are assumed to represent both the fine and coarse fraction. These measurement and modeling studies present lower near-fire deposition impacts than estimated for the hypothetical Los Angeles and Denver scenarios presented here.

Table 2
Modeled hourly maximum ^{137}Cs ambient and deposition levels within 50 km of the fire (column labeled Maximum). The average of all modeled hourly maximum ^{137}Cs within 50 km of the fire is also shown (column labeled Mean).

Scenario	PM mode	Ambient concentration		Deposition	
		Maximum (mBq/m^3)	Mean (mBq/m^3)	Maximum (Bq/m^2)	Mean (Bq/m^2)
Los Angeles	Fine	258	31	82	4
	Coarse	370	36	1118	52
Denver	Fine	459	80	217	8
	Coarse	588	92	4475	123

3.3. Hypothetical scenarios: inhalation exposure

The episode maximum CEDE is shown in Fig. 6 for the Denver and June Los Angeles scenarios. Population CEDE has been expressed as maximum hourly person-μSv-hours for both scenarios. Levels of ^{137}Cs are highest nearest the fire and tend to follow prevailing winds and decrease as distance from the fire increases. Peak predicted population weighted hourly CEDE over all grid cells in the model domain for the Los Angeles scenarios was 24 person-μSv/h and 42 person-μSv/h for the Denver scenario. The difference in ambient levels and population-weighted exposure between the summer and fall Los Angeles scenarios are shown in Fig. S8. Differences in meteorology between these periods resulted in differences in downwind transport of ^{137}Cs and notably different areas of population exposure. In both Los Angeles scenarios, winds transported smoke toward the south but in the fall episode

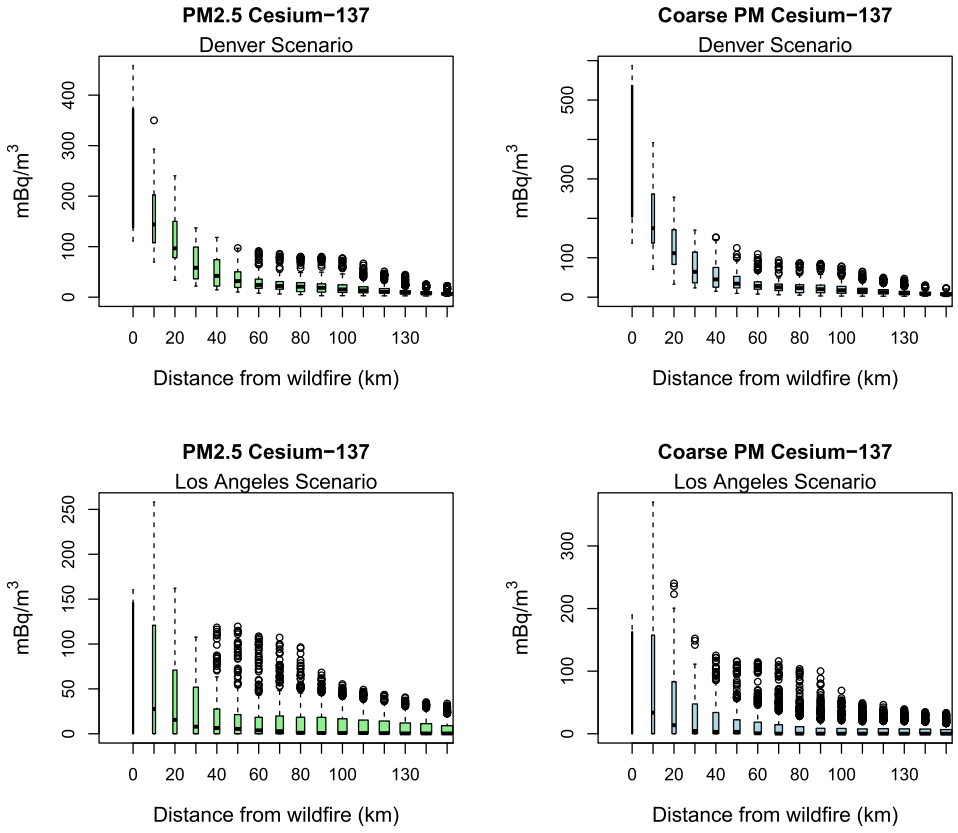

Fig. 4. Distribution of hourly maximum modeled ambient $PM_{2.5}$ and coarse PM ^{137}Cs by distance from the wildfire.

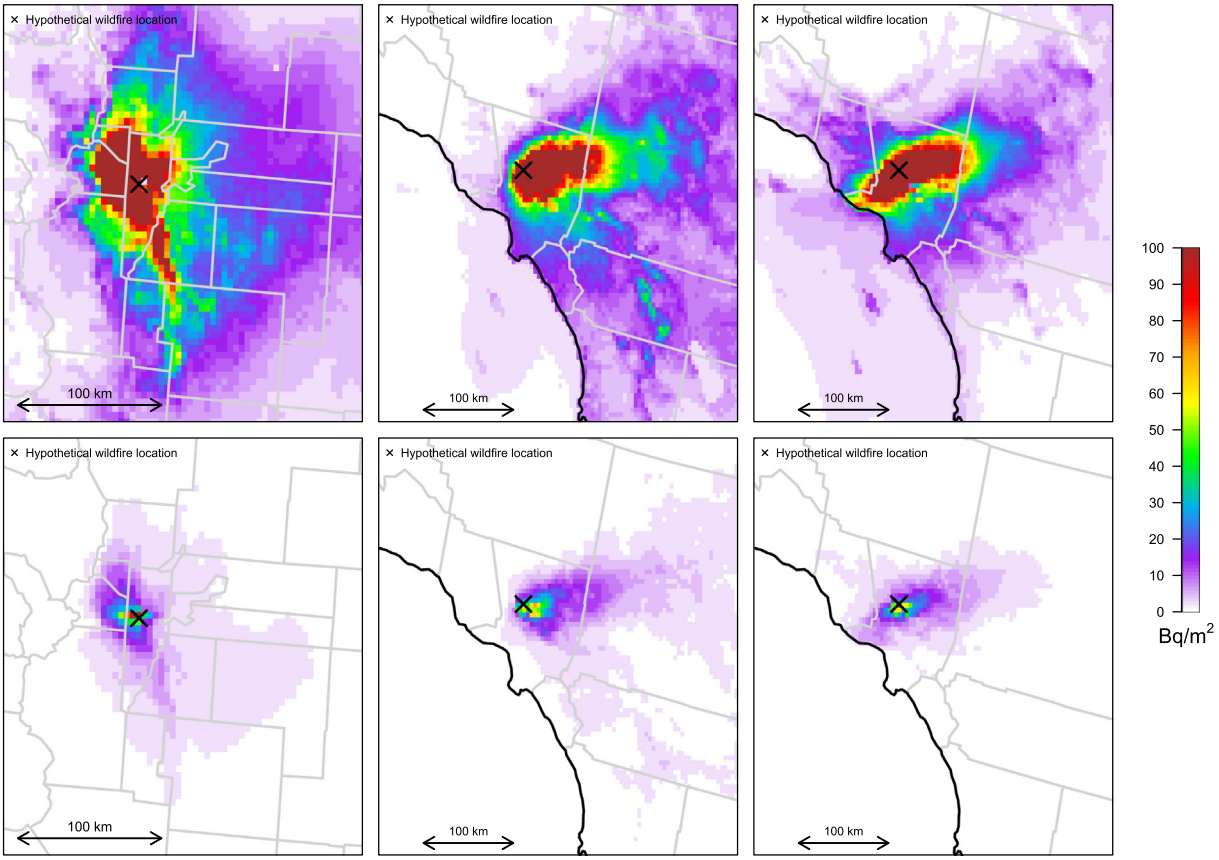

Fig. 5. Episode total modeled dry deposition for ^{137}Cs in coarse (top row) and fine (bottom row) particle modes for the Denver scenario and both Los Angeles scenarios.

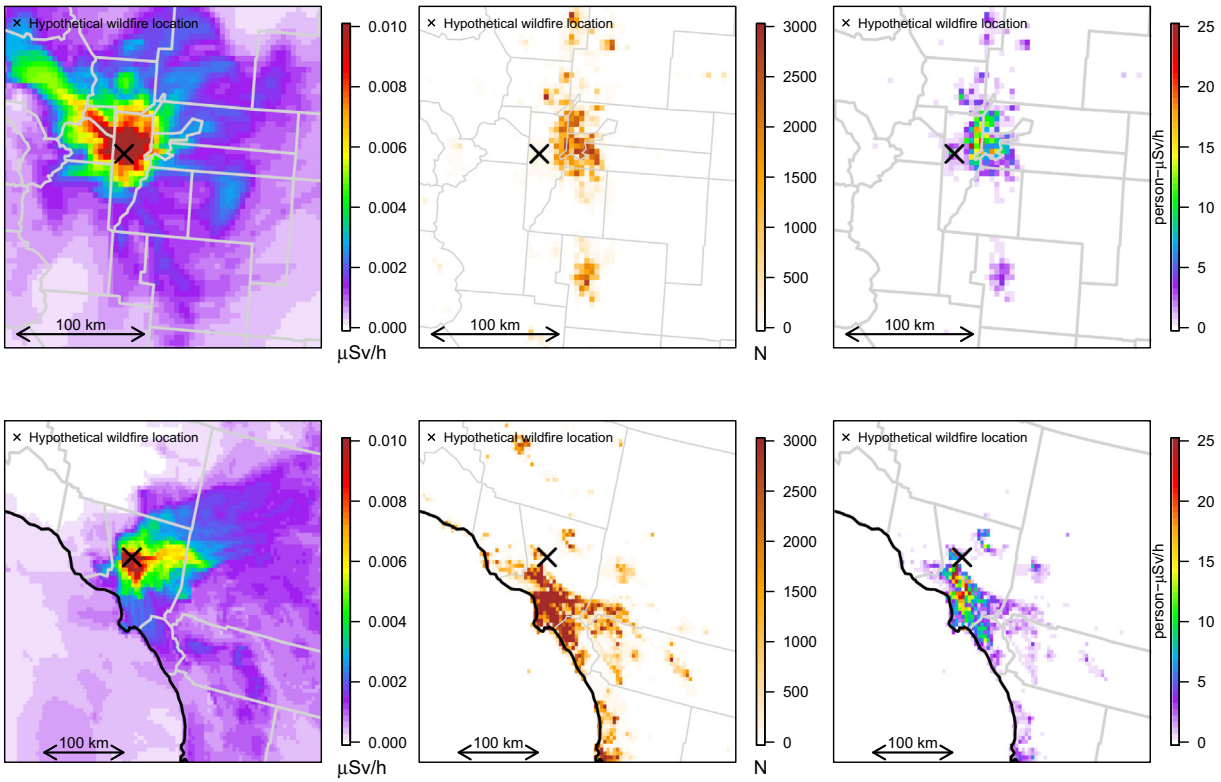

Fig. 6. Episode maximum values of CEDE, population, and population aggregated CEDE shown for the Denver (top row) and June Los Angeles (bottom row) scenarios.

winds tended to expose more people in the northern part of the metropolitan area compared to the summer episode. This suggests that seasonal and even day to day variation in winds would result in somewhat different downwind exposure. Fig. 6 illustrates that the highest ambient concentrations are not always coincident with the highest population exposure. Models provide a useful tool to match predicted concentrations with populations to identify areas to target for priority response. This also demonstrates variability in exposure related to expected variability in winds in this area.

Small 1 km domains were applied for a limited area around each fire scenario to provide a more representative impact for first responders. These simulations were not intended to provide information about downwind population impacts. The near-fire impacts predicted by the 1 km simulation were higher than the 4 km simulation by an approximate factor of 3 for the California scenarios and 4 for the Denver scenario (Fig. S9), which is similar to other grid-model based studies (Baker et al., 2014). This ratio is expected since the 1 km grid cells have a volume that is 4 times smaller than the simulation where 4 km sized grid cells were used. This study suggests peak impacts unpaired in time and space generally match the grid resolution ratio as finer grid resolution tends to result in higher concentrations near a particular source.

4. Conclusions

The modeling system performed well at predicting the timing and often the levels of surface level wildfire smoke impacts on $PM_{2.5}$ organic carbon at routine monitors in California during the summer wildfire season in 2016. Model predicted exposures were below levels necessitating evacuation or sheltering in place which suggests first responders are more likely to have negative health impacts from other pollutants (e.g., carbon monoxide and total $PM_{2.5}$ mass) emitted by wildfire (Adetona et al., 2013) rather than legacy radioactive ^{137}Cs emitted at levels similar to this assessment. Based on other similar assessments in the literature, it is possible that external irradiation from deposited ^{137}Cs could result in a larger exposure than the inhalation pathway assessed here (Hohl et al., 2012).

The downwind CEDE levels predicted by the modeling system suggests that post-fire exposure to a wildfire of the sizes modeled here would not make remediation of forested areas impacted by radiological incidents like the scenarios modeled here a high priority. Certainly, other factors would need to be considered when prioritizing post-incident remediation of forested areas, including the costs of remediation, and resulting damage to the ecosystem.

Laboratory testing of wildfire combustion suggests Cs fate is largely associated with ash (>99%) rather than air emissions (Hao et al., 2018). Future work should consider the impact and potential dose related to ^{137}Cs in ash being mobilized post-fire to groundwater and reservoirs. Future work should also include experiments with actual ^{137}Cs to corroborate the underlying assumption of the laboratory studies that Cs partitioning between coarse and $PM_{2.5}$ is independent of initial Cs concentration.

This work does not provide information about longer-term cumulative dose from other types of post-contamination radiation with longer half-lives (e.g., nuclear weapons testing). The levels presented here may not be relevant for first responders since the model was applied with a horizontal resolution of 1 km using meteorology and terrain interpolated from a coarser 4 km dataset. These near-fire findings should be corroborated with future work using more highly resolved input data. Further, additional information about ^{137}Cs emissions in non-litter fuels (e.g., woody growth) and how much contaminated ash would be emitted as part of the convective updrafts typical for larger wildfires would provide an improved representation of wildfire redistribution of legacy radionuclides.

The CEDE provided in this assessment were not adjusted for use of personal protective equipment. Finer resolution modeling could result in higher CEDE while personal protective equipment would likely reduce CEDE for first responders and downwind impacted population. Future research could include other radionuclides that could result in higher CEDE

with lower concentrations (e.g., alpha emitters) would be a useful compliment to this assessment. Further, future work could include additional exposure pathways such as ingestion of contaminated food or external radiation from the ground through newly deposited radionuclides.

Disclaimer

The views expressed in this article are those of the authors and do not necessarily represent the views or policies of the U.S. Environmental Protection Agency. The U.S. Environmental Protection Agency through its Office of Research and Development and Office of Air and Radiation funded, managed, and collaborated in the research described here under contract EP-D-11-006, Work Assignment 5–14 with Eastern Research Group, GSA Task Order No. ID04160145 "EPA Air Quality Modeling and Simulation Analysis", and Interagency Agreement DW-12-92,437,601-0 with the U.S. Forest Service. It has been subjected to the Agency's review and has been approved for publication. Note that approval does not signify that the contents necessarily reflect the views of the Agency. Mention of trade names, products, or services does not convey official EPA approval, endorsement, or recommendation.

CRediT authorship contribution statement

Kirk R. Baker: Conceptualization, Methodology, Writing – original draft, Data curation, Investigation, Writing – review & editing. **Sang Don Lee:** Conceptualization, Methodology, Data curation, Investigation, Writing – review & editing. **Paul Lemieux:** Conceptualization, Methodology, Data curation, Investigation, Writing – review & editing. **Scott Hudson:** Methodology, Investigation, Writing – review & editing. **Benjamin N. Murphy:** Software, Writing – review & editing. **Jesse O. Bash:** Software, Data curation. **Shannon N. Koplitz:** Formal analysis, Investigation. **Thien Khoi V. Nguyen:** Formal analysis, Writing – review & editing. **Wei Min Hao:** Data curation. **Stephen Baker:** Data curation. **Emily Lincoln:** Data curation.

Declaration of competing interest

The authors declare that they have no known competing financial interests or personal relationships that could have appeared to influence the work reported in this paper.

Acknowledgements

The authors would like to recognize the contributions of James Beidler, Barron Henderson, Chris Allen, Lara Reynolds, Andrew Langford, Christoph Senff, Raul Alvarez, David Stuenkel, and Sara DeCair.

Supplementary data

Supplementary data to this article can be found online at https://doi.org/10.1016/j.scitotenv.2021.148872.

References

Abatzoglou, J.T., Williams, A.P., 2016. Impact of anthropogenic climate change on wildfire across western US forests. Proc. Natl. Acad. Sci. 113, 11770–11775.

Adetona, O., Simpson, C.D., Onstad, G., Naeher, L.P., 2013. Exposure of wildland firefighters to carbon monoxide, fine particles, and levoglucosan. Ann. Occup. Hyg. 57, 979–991.

Appel, K., Pouliot, G., Simon, H., Sarwar, G., Pye, H., Napelenok, S., Akhtar, F., Roselle, S., 2013. Evaluation of dust and trace metal estimates from the Community Multiscale Air Quality (CMAQ) model version 5.0. Geosci. Model Dev. 6, 883–899.

Appel, K.W., Bash, J.O., Fahey, K.M., Foley, K.M., Gilliam, R.C., Hogrefe, C., Hutzell, W.T., Kang, D., Mathur, R., Murphy, B.N., 2020. The Community Multiscale Air Quality (CMAQ) model versions 5.3 and 5.3. 1: system updates and evaluation. Geosci. Model Dev. Discuss. 1–41.

Baker, K.R., Misenis, C., Obland, M.D., Ferrare, R.A., Scarino, A.J., Kelly, J.T., 2013. Evaluation of surface and upper air fine scale WRF meteorological modeling of the May and June 2010 CalNex period in California. Atmos. Environ. 80, 299–309.

Baker, K.R., Hawkins, A., Kelly, J.T., 2014. Photochemical grid model performance with varying horizontal grid resolution and sub-grid plume treatment for the Martins Creek near-field SO 2 study. Atmos. Environ. 99, 148–158.

Baker, K., Carlton, A., Kleindienst, T., Offenberg, J., Beaver, M., Gentner, D., Goldstein, A., Hayes, P., Jimenez, J., Gilman, J., 2015. Gas and aerosol carbon in California: comparison of measurements and model predictions in Pasadena and Bakersfield. Atmos. Chem. Phys. 15, 5243–5258.

Baker, K., Woody, M., Tonnesen, G., Hutzell, W., Pye, H., Beaver, M., Pouliot, G., Pierce, T., 2016. Contribution of regional-scale fire events to ozone and PM 2.5 air quality estimated by photochemical modeling approaches. Atmos. Environ. 140, 539–554.

Baker, K., Woody, M., Valin, L., Szykman, J., Yates, E., Iraci, L., Choi, H., Soja, A., Koplitz, S., Zhou, L., 2018. Photochemical model evaluation of 2013 California wild fire air quality impacts using surface, aircraft, and satellite data. Sci. Total Environ. 637, 1137–1149.

Bash, J.O., Baker, K.R., Beaver, M.R., 2016. Evaluation of improved land use and canopy representation in BEIS v3. 61 with biogenic VOC measurements in California. Geosci. Model Dev. 9, 2191.

Bourcier, L., Sellegri, K., Masson, O., Zangrando, R., Barbante, C., Gambaro, A., Pichon, J.-M., Boulon, J., Laj, P., 2010. Experimental evidence of biomass burning as a source of atmospheric 137Cs, puy de Dôme (1465 m asl), France. Atmos. Environ. 44, 2280–2286.

Browne, E., Tuli, J., 2007. Nuclear data sheets for A = 137. Nucl. Data Sheets 108, 2173–2318.

Commodore, A.A., Jannik, G.T., Eddy, T.P., Rathbun, S.L., Hejl, A.M., Pearce, J.L., Irvin-Barnwell, E.A., Naeher, L.P., 2012. Radioactivity in smoke particulates from prescribed burns at the Savannah River Site and at selected southeastern United States forests. Atmos. Environ. 54, 643–656.

Connell, R., 2012. Wide Area Recovery and Resiliency Program (WARRP) Interim Clearance Strategy for Environments Contaminated with Cesium-137. Environmental Protection Agency Washington DC.

Dennison, P.E., Brewer, S.C., Arnold, J.D., Moritz, M.A., 2014. Large wildfire trends in the western United States, 1984–2011. Geophys. Res. Lett. 41, 2928–2933.

Eckerman, K.F., Wolbarst, A.B., Richardson, A.C., 1988. Limiting Values of Radionuclide Intake and Air Concentration and Dose Conversion Factors for Inhalation, Submersion, and Ingestion: Federal Guidance Report No. 11. Environmental Protection Agency, Washington, DC (USA). Office of Radiation.

Faloona, I.C., Chiao, S., Eiserloh, A.J., Alvarez, R.J., Kirgis, G., Langford, A.O., Senff, C.J., Caputi, D., Hu, A., Iraci, L.T., 2020. The California Baseline Ozone Transport Study (CABOTS). Bull. Am. Meteorol. Soc. 101, E427–E445.

Flocke, F., Pfister, G., Crawford, J.H., Pickering, K.E., Pierce, G., Bon, D., Reddy, P., 2020. Air quality in the northern Colorado front range metro area: the front range air pollution and photochemistry Éxperiment (FRAPPÉ). J. Geophys. Res.-Atmos. 125 (e2019JD031197).

Garten Jr., C.T., Hamby, D., Schreckhise, R., 2000. Radiocesium discharges and subsequent environmental transport at the major US weapons production facilities. Sci. Total Environ. 255, 55–73.

Goldammer, J.G., Statheropoulos, M., Andreae, M.O., 2008. Impacts of vegetation fire emissions on the environment, human health, and security: a global perspective. Dev. Environ. Sci. 8, 3–36.

Hao, W.M., Baker, S., Lincoln, E., Hudson, S., Lee, S.D., Lemieux, P., 2018. Cesium emissions from laboratory fires. J. Air Waste Manage. Assoc. 68, 1211–1223.

Harper, M., Butler, C., Berry, D., Wroble, J., 2015. Where occupation and environment overlap: US forest service worker exposure to libby amphibole fibers. J. Occup. Environ. Hyg. 12, D47–D53.

Hashimoto, S., Ugawa, S., Nanko, K., Shichi, K., 2012. The total amounts of radioactively contaminated materials in forests in Fukushima, Japan. Sci. Rep. 2, 416.

Hohl, A., Niccolai, A., Oliver, C., Melnychuk, D., Zibtsev, S., Goldammer, J.G., Gulidov, V., 2012. The human health effects of radioactive smoke from a catastrophic wildfire in the Chernobyl Exclusion Zone: a worst case scenario. International Scientific Electronic Journal Earth Bioresources and Life Quality Founded by National University of Life and Environmental Sciences of Ukraine (NUBiP of Ukraine) and Global Consortium of Higher Education and Research for Agriculture (GCHERA), p. 1.

IAEA, 2011. Radiation protection and safety of radiation sources: international basic safety standards: general safety requirements. Vienna: International Atomic Energy Agency, General Safety Requirements Part 3, 2011, Interim edition https://www-pub.iaea.org/MTCD/Publications/PDF/p1531interim_web.pdf.

Imamura, N., Komatsu, M., Ohashi, S., Hashimoto, S., Kajimoto, T., Kaneko, S., Takano, T., 2017. Temporal changes in the radiocesium distribution in forests over the five years after the Fukushima Daiichi Nuclear Power Plant accident. Sci. Rep. 7, 8179.

Jouve, A., Schulte, E., Bon, P., Cardot, A., 1993. Mechanical and physical removing of soil and plants as agricultural mitigation techniques. Sci. Total Environ. 137, 65–79.

Kashparov, V., Lundin, S., Kadygrib, A., Protsak, V., Levtchuk, S., Yoschenko, V., Kashpur, V., Talerko, N., 2000. Forest fires in the territory contaminated as a result of the Chernobyl accident: radioactive aerosol resuspension and exposure of fire-fighters. J. Environ. Radioact. 51, 281–298.

Kelly, J.T., Baker, K.R., Nolte, C.G., Napelenok, S.L., Keene, W.C., Pszenny, A.A., 2016. Simulating the phase partitioning of NH 3, HNO 3, and HCl with size-resolved particles over northern Colorado in winter. Atmos. Environ. 131, 67–77.

Knepp, T.N., Szykman, J.J., Long, R., Duvall, R.M., Krug, J., Beaver, M., Cavender, K., Kronmiller, K., Wheeler, M., Delgado, R., 2017. Assessment of mixed-layer height estimation from single-wavelength ceilometer profiles. Atmos. Meas. Tech. 10, 3963.

Kristensen, L.J., Taylor, M.P., Odigie, K.O., Hibdon, S.A., Flegal, A.R., 2014. Lead isotopic compositions of ash sourced from Australian bushfires. Environ. Pollut. 190, 159–165.

Langford, A.O., Alvarez, I.I.R.J., Kirgis, G., Senff, C.J., Caputi, D., Conley, S.A., Faloona, I.C., Iraci, L.T., Marrero, J.E., McNamara, M.E., 2019. Intercomparison of lidar, aircraft, and surface ozone measurements in the San Joaquin Valley during the California Baseline Ozone Transport Study (CABOTS). Atmos. Meas. Tech. 12, 1889–1904.

Larkin, N., Raffuse, S., Huang, S., Pavlovic, N., Rao, V., 2020. The comprehensive fire information reconciled emissions (CFIRE) inventory: wildland fire emissions developed for the 2011 and 2014 US National Emissions Inventory. J. Air Waste Manage. Assoc. 70 (11), 1165–1185.

Li, R., Wiedinmyer, C., Baker, K., Hannigan, M., 2013. Characterization of coarse particulate matter in the western United States: a comparison between observation and modeling. Atmos. Chem. Phys. 13, 1311.

Linkov, I., Morel, B., Schell, W.R., 1997. Remedial policies in radiologically-contaminated forests: environmental consequences and risk assessment. Risk Anal. 17, 67–75.

Nolte, C., Appel, K., Kelly, J., Bhave, P., Fahey, K., Collett Jr., J., Zhang, L., Young, J., 2015. Evaluation of the Community Multiscale Air Quality (CMAQ) model v5. 0 against size-resolved measurements of inorganic particle composition across sites in North America. Geosci. Model Dev. 8, 2877–2892.

Paatero, J., Vesterbacka, K., Makkonen, U., Kyllönen, K., Hellen, H., Hatakka, J., Anttila, P., 2009. Resuspension of radionuclides into the atmosphere due to forest fires. J. Radioanal. Nucl. Chem. 282, 473–476.

Reid, C.E., Brauer, M., Johnston, F.H., Jerrett, M., Balmes, J.R., Elliott, C.T., 2016. Critical review of health impacts of wildfire smoke exposure. Environ. Health Perspect. 124, 1334–1343.

Saffarzadeh, A., Shimaoka, T., Kakuta, Y., Kawano, T., 2014. Cesium distribution and phases in proxy experiments on the incineration of radioactively contaminated waste from the Fukushima area. J. Environ. Radioact. 136, 76–84.

Schoennagel, T., Balch, J.K., Brenkert-Smith, H., Dennison, P.E., Harvey, B.J., Krawchuk, M.A., Mietkiewicz, N., Morgan, P., Moritz, M.A., Rasker, R., 2017. Adapt to more wildfire in western North American forests as climate changes. Proc. Natl. Acad. Sci. 114, 4582–4590.

Senff, C., Langford, A., Alvarez, R., Bonin, T., Brewer, A., Choukulkar, A., Kirgis, G., Marchbanks, R., Sandberg, S., Weickmann, A., 2020. Entrainment and Mixing of Transported Ozone Layers: Implications for Surface Air Quality in the Western US, EPJ Web of Conferences. EDP Sciences.

Skamarock, W.C., Klemp, J.B., Dudhia, J., Gill, D.O., Barker, D.M., Wang, W., Powers, J.G., 2005. A description of the advanced research WRF version 2. National Center For Atmospheric Research Boulder Co Mesoscale and Microscale.

Strode, S.A., Ott, L.E., Pawson, S., Bowyer, T.W., 2012. Emission and transport of cesium-137 from boreal biomass burning in the summer of 2010. J. Geophys. Res.-Atmos. 117.

Takada, M., Yamada, T., Takahara, T., Okuda, T., 2016. Spatial variation in the 137Cs inventory in soils in a mixed deciduous forest in Fukushima, Japan. J. Environ. Radioact. 161, 35–41.

Tikhomirov, F., Shcheglov, A., 1994. Main investigation results on the forest radioecology in the Kyshtym and Chernobyl accident zones. Sci. Total Environ. 157, 45–57.

U.S. Environmental Protection Agency, 2018. 2014 National Emissions Inventory, version 2 technical support document. https://www.epa.gov/sites/production/files/2018-07/documents/nei2014v2_tsd_05jul2018.pdf.

U.S. Forest Service, 2019. The fuel characteristic classification system. https://www.fs.fed.us/pnw/fera/fft/fccsmodule.shtml.

Viner, B.J., Jannik, T., Stone, D., Hepworth, A., Naeher, L., Adetona, O., Blake, J., Eddy, T., 2015. Modelling and mitigating dose to firefighters from inhalation of radionuclides in wildland fire smoke. Int. J. Wildland Fire 24, 723–733.

Wiedinmyer, C., Friedli, H., 2007. Mercury emission estimates from fires: an initial inventory for the United States. Environ. Sci. Technol. 41, 8092–8098.

Wotawa, G., De Geer, L.E., Becker, A., D'Amours, R., Jean, M., Servranckx, R., Ungar, K., 2006. Inter-and intra-continental transport of radioactive cesium released by boreal forest fires. Geophys. Res. Lett. 33.

Yoschenko, V., Kashparov, V., Levchuk, S., Glukhovskiy, A., Khomutinin, Y.V., Protsak, V., Lundin, S., Tschiersch, J., 2006. Resuspension and redistribution of radionuclides during grassland and forest fires in the Chernobyl exclusion zone: part II. Modeling the transport process. J. Environ. Radioact. 87, 260–278.

Zhou, L., Baker, K.R., Napelenok, S.L., Pouliot, G., Elleman, R., O'Neill, S.M., Urbanski, S.P., Wong, D.C., 2018. Modeling crop residue burning experiments to evaluate smoke emissions and plume transport. Sci. Total Environ. 627, 523–533.

Zhu, Y.G., Smolders, E., 2000. Plant uptake of radiocaesium: a review of mechanisms, regulation and application. J. Exp. Bot. 51, 1635–1645.